

Eyring acceleration model for predicting calendar ageing of lithium-ion batteries

Eduardo Redondo-Iglesias, Pascal Venet, Serge Pelissier

▶ **To cite this version:**

Eduardo Redondo-Iglesias, Pascal Venet, Serge Pelissier. Eyring acceleration model for predicting calendar ageing of lithium-ion batteries. Journal of Energy Storage, 2017, 13, pp.176-183. 10.1016/j.est.2017.06.009 . hal-01575005

HAL Id: hal-01575005
https://hal.science/hal-01575005

Submitted on 17 Aug 2017

HAL is a multi-disciplinary open access archive for the deposit and dissemination of scientific research documents, whether they are published or not. The documents may come from teaching and research institutions in France or abroad, or from public or private research centers.

L'archive ouverte pluridisciplinaire **HAL**, est destinée au dépôt et à la diffusion de documents scientifiques de niveau recherche, publiés ou non, émanant des établissements d'enseignement et de recherche français ou étrangers, des laboratoires publics ou privés.

https://doi.org/10.1016/j.est.2017.06.009

Eyring acceleration model for predicting calendar ageing of lithium-ion batteries.

Eduardo Redondo-Iglesias[a,b,*], Pascal Venet[b], Serge Pelissier[a]

[a] *Univ Lyon, IFSTTAR, AME, LTE, 69500 Bron, France*
[b] *Univ Lyon, UCB Lyon 1, AMPERE UMR CNRS 5005, 69100 Villeurbanne, France*

Abstract

Modelling of lithium-ion batteries calendar ageing is often based on a semi-empirical approach by using, for example the Arrhenius acceleration model. Our approach is based on Eyring acceleration model, which is not widely used for electrochemical energy storage components. Parameter identification is typically performed without taking into account the state-of-charge (SoC) drifting. However, even in rest condition, battery cells' SoC drifts because of capacity losses (self-discharge and capacity fade). In this work we have taken into account the SoC drift during calendar ageing tests. For this, we considered available capacity (Ah) instead of SoC (%) as ageing factor. Then, the analytical solution of the problem leads to the use of the Lambert W function in the model formulation. Simulation results show that Lambert-Eyring model is more accurate and allows a reduction in the number of parameters to be identified.

Keywords: Lithium-ion battery, reliability, accelerated ageing, modelling, Eyring Law, Lambert W function

NOMENCLATURE

SoC	State of Charge
T	Temperature
Q_0	Initial capacity
Q	Current capacity
Q_a	Available capacity
Q_d	Used capacity
Q_{sd}	Self-discharge (reversible capacity loss)
Q_L	Capacity fade (irreversible capacity loss)

1. Introduction

During the last decade, electric vehicles (EV) and hybrid electric vehicles sales have grown from 0.1 to 3% in France [1]. However, the low range and high purchasing price of EV's are the main obstacles to their market penetration. Range and price are directly related to the battery size which is the most expensive component of an electric vehicle. Currently, car manufacturers have found a compromise between price and range that fixes typically the range between 100 and 200 km for a purchasing price (including batteries) from 20 to 40 k€. Battery size of those vehicles vary from 16 to 24 kWh.

Electric vehicles can contribute to a cleaner mobility, but for this, the whole life cycle must be optimized in order to be less resource consumer and less waste producer than thermal vehicles.

Energy management of the vehicle is often optimized with an energy economy aim, but it can also be done for extending the battery longevity. The elaboration of this kind of strategies requires reliable and accurate ageing models.

In this paper, calendar ageing of lithium-ion LFP/C cells has been modelled. Calendar ageing seems to be predominant in batteries used in applications such as electric vehicle. LFP cells offer high durability, power and safety, which represent three crucial performances for transportation applications.

A classical approach of model parameter identification consists on a step by step identification: first step consists of identifying the temperature (T) influence and then the second step is for the state-of-charge (SoC) influence. For this, every factor (T and SoC) must be considered as being constant.

During calendar ageing tests, constant tempera-

*Corresponding author: eduardo.redondo@ifsttar.fr

ture is easily driven because battery cells are in rest condition and no heat is emitted by them. However, battery cells' SoC is not constant: SoC drifts over time because of capacity losses.

Consequently, SoC drift may be considered from the parameter identification phase in order to improve the ageing model accuracy. The chosen formulation in this work relies on the Eyring acceleration law [2]. This law allows a global approach where all parameters can be identified in a single step.

2. Calendar ageing

Calendar ageing of a battery cell is the degradation of its performances while being in rest condition, that is when no current is supplied or absorbed by this cell. This type of ageing must considered in transport applications because vehicles are parked 95% of the time [3].

Calendar ageing yields on ageing mechanisms caused by side reactions between the different chemical substances inside each component of the battery (electrodes, electrolyte, etc.). Ageing mechanisms of lithium-ion batteries are numerous, complex and can interact with each other [4].

As on battery cells the main ageing mechanisms lie on chemical reactions, the battery performances degrade over time as these reactions advance. Thus, Arrhenius-like laws are commonly used to explain the thermal stress influence on performances. Equation 1 is a general form for a performance ($y(t)$) degrading over time under a thermal stress (T) using the modified Arrhenius law. The performance $y(t)$ can be the internal resistance (power fade) [5–8] or the capacity fade [9–11] with T the absolute temperature (in K), A the pre-exponential factor, E_a the activation energy for the reaction (in eV), k the Boltzmann constant and $f(t)$ the time degradation function of $y(t)$ considered.

$$y(t) = AT^n e^{(Ea/kT)} f(t) \tag{1}$$

The Eyring law is also used on reliability studies [2] for example for mechanical components [12]. This law extends the Arrhenius law to other stress factors S_i such as pressure, current, voltage, etc. Equation 2 is a general form for a performance ($y(t)$) degrading over time under two type of stresses (T and S_i) using the Eyring law. In the Eyring law each additional stress is added to the exponential function beside the thermal stress term (E_a/kT). The direct influence of a stress is B_iS_i and C_iS_i/kT represent an interaction term between temperature and S_i where B_i, C_i are stress-dependent constants.

$$y(t) = AT^n e^{(Ea/kT + B_iS_i + C_iS_i/kT)} f(t) \tag{2}$$

In this paper, we have modelled calendar ageing of A123 LFP/C cells (2.3Ah) from SIMCAL project [13]. The main calendar ageing mechanism in this type of cells is SEI (Solid Electrolyte Interface) formation [14]. The consequence of this ageing mechanism is the capacity fade due to a loss of lithium inventory.

In order to facilitate the results comparison, all capacity measurements and simulation are expressed relative to initial capacity (p.u.).

2.1. Accelerated ageing tests in SIMCAL project

Accelerated ageing tests were carried out in order to show up the ageing mechanisms responsible of battery degradation. These tests consist in putting battery cells to different levels of use constraints. The collected results can be used afterwards to establish remaining useful life or performance evolution laws.

In the case of calendar ageing, two factors have been identified as being responsible of battery degradation: temperature (T) and state-of-charge (SoC). In SIMCAL project [13], six technologies of batteries (one NMC/C, one NCA/C, one LMO/NMC blended/C and three LFP/C) were tested to study the influence of SoC and temperature as ageing factors. Target values of factors are 30, 45 and 60° C for temperature and 30, 65 and 100% for SoC. Each couple of values (T, SoC) was assigned to three different cells to improve the representativeness of the results. Cells' performances were periodically measured by the means of RPTs (Reference Performance Tests) at 25° C. The RPT protocol consisted in:

- Full charge/discharge cycle at 1C rate for capacity measurement
- Electrochemical Impedance Spectroscopy (EIS) and time response to pulse profiles at different values of SoC

In this work, we focused the analysis to one LFP/C technology and exploited only the capacity measurements.

Figure 1 shows the capacity loss evolution (Q_L) of A123 cells from SIMCAL project. In this figure the temperature influence is clearly perceptible: if cells are grouped by SoC level, cell degradation is greater at higher temperatures (that is, degradation rate is higher for 60° C than for 45° C and than for 30° C for each SoC level).

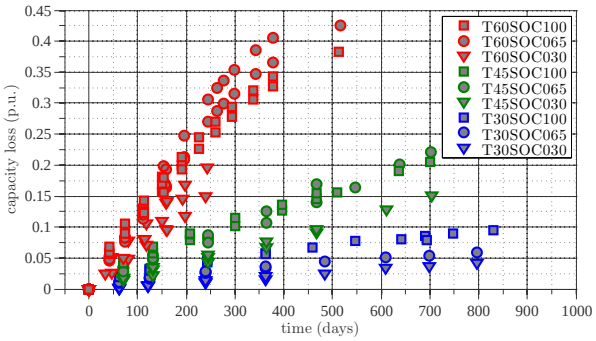


Figure 1: Capacity loss of A123 cells from SIMCAL project.

Nonetheless, the reciprocity of this sentence is not always true: the degradation rate is not always higher at higher SoC levels. At 30° C cell degradation is greater when SoC is higher, that is degradation at SoC 100% is higher than when SoC is 65% and 30%. However, at 45° C, degradation at SoC 100% is similar than when SoC is 65%. Even at 60° C, degradation at SoC 100% is lower than when SoC is 65%. This behaviour seems to be atypical and highlights a strong interaction between the ageing factors (T, SoC).

2.2. SoC drift during ageing tests

When a battery cell is at rest condition, its energy (capacity) and power (impedance) performances change by ageing. Cell's SoC changes also. SoC drift of a cell in rest is caused by capacity losses. Capacity losses are either reversible, due to self-discharge; either irreversible, due to degradation mechanisms.

SoC (expressed in p.u.) is defined in equation 3 as the ratio between available quantity of charge (Q_a) and current capacity (Q) at every moment (t):

$$SoC(t) = \frac{Q_a(t)}{Q(t)} \tag{3}$$

Q_a can be expressed as a function of discharged quantity of charge (Q_d) since the last full charge and self-discharge (Q_{sd}) as shown in equation 4:

$$Q_a(t) = Q(t) - Q_d(t) - Q_{sd}(t) \tag{4}$$

On the other hand, cell capacity change according to ageing (equation 5), Q_0 and Q_L are respectively initial capacity and irreversible capacity loss:

$$Q(t) = Q_0 - Q_L(t) \tag{5}$$

These three equations lead to the following expression for SoC evolution:

$$SoC(t) = \left(1 - \frac{Q_d(t) + Q_{sd}(t)}{Q_0 - Q_L(t)}\right) \tag{6}$$

Equation 6 highlights that SoC is not constant during the rest phase between two RTPs and that SoC drift occurs during ageing tests. The drift is mainly caused by capacity fade (Q_L) as self-discharge (Q_{sd}) is relatively low and often negligible for lithium-ion batteries. With ageing, Q_L increases and to maintain SoC constant during the test, one should change the value of Q_d. Q_d is the quantity of charge discharged after a RPT from the cell at SoC 100% to put it at the target SoC (65 or 30%). For commodity reasons the same value of Q_d is used all along the duration of the experiments. Otherwise, one should compute a new value of Q_d for each cell after each RTP which is practically infeasible when hundreds of cells are tested. For this reason a cell supposed to be stored for instance at SoC 65% is effectively stored at this value only at the beginning of the experiments. As soon as an irreversible capacity fade occurs, the storage SoC drifts.

Figure 2 shows SoC drift of battery cells as a function of irreversible capacity losses (Q_L) in the absence of self-discharge ($Q_{sd} = 0$). In this figure, SoC drift is calculated as in equation 6 for three different initial values of SoC (30, 65 and 100%), so Q_d is respectively 0.7, 0.35 and 0 p.u. Therefore, even if no self-discharge takes place, SoC inevitably drifts away from the desired SoC level. This SoC drift is a source of imprecision if it is not taken into account when identifying the model parameters.

SoC drift is minimal when target SoC is 100%. Experimental data reveal that SoC drift in SoC100 cells was lower than 3%.

3. Ageing modelling

As explained above, lithium-ion battery ageing depends mainly of the couple (T, SoC). During the ageing tests, each cell has been stored at couple

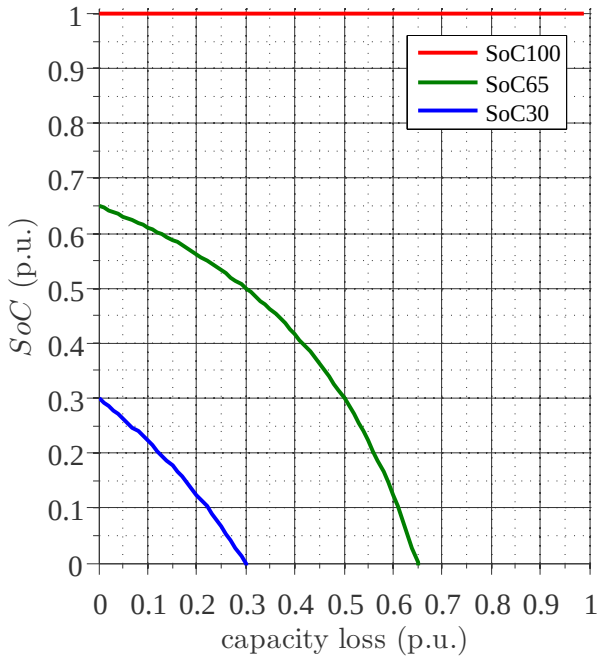


Figure 2: SoC drift according to expression 6 with $Q_{sd} = 0$.

of values (T, SoC), but SoC drifts mainly because of capacity losses (Q_L).

At first, in order to model the battery ageing, a variable reflecting the battery degradation must be chosen. This variable can be, for example, the cell impedance [5, 15] or the derivative of capacity over time ($\frac{dQ_L}{dt}$) [16]. In this work, we have chosen to model the capacity fade evolution (Q_L) which is the key parameter in EV applications.

Equation 7 is a generic example of Q_L ageing model as a function of t, T and SoC where the ageing factors (T, SoC) are decoupled from time [17]:

$$Q_L(t, T, SoC) = C_A(T, SoC) \cdot f(t) \quad (7)$$

This equation implies that Q_L evolution for every cell follows the same shape ($f(t)$) independently of the value of T and SoC. T and SoC will change the size of the shape with an acceleration coefficient (C_A).

Typically, the chosen $f(t)$ is a power of time (t^z) [5], an exponential function [15] or a composition of time functions [18], for example ($t + \sqrt{t}$).

3.1. Ageing model without taking into account the SoC drift

The classical approach to ageing modelling consists in expressing C_A with an Arrhenius expression [5, 6]. Pre-exponential factor (A) and activation energy (E_a) of the Arrhenius law may change in terms of the other ageing factors. So, for calendar ageing, these two parameters are expressed as a function of SoC: $A = A(SoC)$, $E_a = E_a(SoC)$.

In this work the chosen shape function $f(t)$ is t^z with a fixed z independently of T and SoC. In this paper the model has been studied with two different values of z: 0.5 and 1. Equation 8 is the ageing model general equation, where k is the Boltzmann constant.

$$Q_L(t, T, SoC) = A(SoC) \cdot e^{\left(-\frac{E_a(SoC)}{k \cdot T}\right)} t^z \quad (8)$$

Once the model general equation is established, the next step consists in identifying the parameter values A and E_a at each SoC level. This is only possible if SoC is assumed to be constant (100, 65 or 30) for each cell throught the ageing tests. This is equivalent to model separately the cells corresponding to each SoC (that is, to find an ageing model for each SoC level).

Figure 3 shows three couples of values (A, E_a) identified for two values of z.

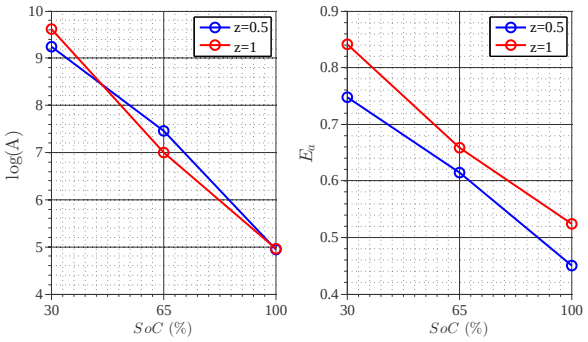
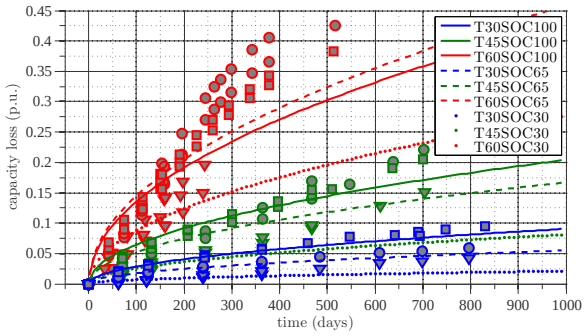


Figure 3: Arrhenius parameter identification as a function of SoC.

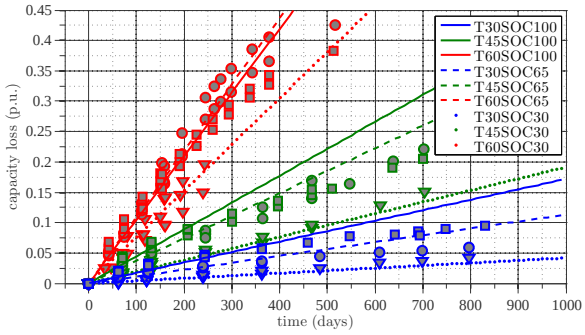
At the end of the first step, we have three ageing models that depend of temperature; one model for each SoC level (30, 65, 100), characterized by their parameter values: (A_{30}, E_{a30}), (A_{65}, E_{a65}) and (A_{100}, E_{a100}).

Second step consists in aggregating these three models in only one model and extrapolating in the whole domain of SoC (0 - 100). Figure 3 shows that $log(A)$ and E_a are mainly linearly dependent of SoC. So, a linear regression can be performed on the previously identified values to obtain the parameters A_0, B_s, E_{a0} and C_s:

$$log(A(SoC)) = log(A_0) + B_s \cdot SoC \quad (9)$$



(a) Model 1 ($z = 0.5$).



(b) Model 1' ($z = 1$).

Figure 4: Simulation results of the model without taking into account the SoC drift (factors: T, SoC). Caption for experimental points are the same that in figure 1.

$$A(SoC) = A_0 e^{B_s \cdot SoC} \tag{10}$$

$$E_a(SoC) = E_{a0} + C_s \cdot SoC \tag{11}$$

By replacing 10 and 11 in 8, we obtain equation 12:

$$Q_L(t, T, SoC) = A_0 e^{B_s \cdot SoC} \cdot e^{\left(-\frac{E_{a0} + C_s \cdot SoC}{k \cdot T}\right)} t^z \tag{12}$$

The identification results are collected in table 1 (model 1: $z = 0.5$ and model 1': $z = 1$). For each linear regression, the coefficients of determination (r^2) are higher than 0.99, independently of the value of z.

Figure 4 illustrates the simulations results of the ageing model compared to measurements. When the chosen shape function is $\sqrt{t}$ ($z = 0.5$, 4a), model generally underestimates ageing; on the contrary, the simulations are rather divergent when $z = 1$ (linear evolution of capacity fade over time, 4b).

3.2. Ageing model taking into account the SoC drift

When one ageing acceleration factor, SoC, is variable over time, the parameter identification of the model is not feasible in several steps as previously. The model general equation must be expressed as a function of all the ageing factors before the identification phase, in order to perform a one single step parameter identification. For this reason, we have decided to use the Eyring model.

Table 1: Identified parameter values: models 1 and 1'.

model	z (no units)	A_0 (p.u./day^z)	B_s (no units)	E_{a0} (eV)	C_s (eV)
1	0.5	$1.65 \cdot 10^{11}$	$-6.16 \cdot 10^{-2}$	0.880	$-4.24 \cdot 10^{-3}$
1′	1	$3.22 \cdot 10^{11}$	$-6.64 \cdot 10^{-2}$	0.969	$-4.52 \cdot 10^{-3}$

Eyring law [2] is an extension of Arrhenius law [19] (temperature dependent) to other stress constraints S_i. Eyring formulation has already been used to model the remaining useful life of materials and mechanical components [12], but is not still widely used for electrochemical energy storage systems. Some recent works propose the Eyring model to express the ageing laws of supercapacitors [20, 21] and batteries [17, 22].

For supercapacitors and other electrical components, the chosen ageing factors are mainly temperature and voltage (T, U) meanwhile ageing modelling of batteries is expressed as a function of the state-of-charge (SoC) instead of the voltage.

When taking into account the SoC drift, we realize that SoC dependence with capacity loss (Q_L) is not linear and could lead to an inextricable formulation. That is the reason why we have proposed available capacity (Q_a) instead of SoC as ageing factor because of its linearity relation with Q_L, as indicated by equations 4 and 5. Shape function $f(t)$ is the same as in the previous section: t^z.

By taking equation 7 and expressing C_A according to an Eyring law depending of T and Q_a, we obtain the ageing model general equation 13. However, we will firstly study a particular case of the Eyring law where n and C are 0 (equation 14).

$$Q_L(t, T, Q_a) = A \cdot T^n \cdot e^{\left(-\frac{E_a}{k \cdot T} + (B + \frac{C}{kT}) \cdot Q_a\right)} t^z \tag{13}$$

$$Q_L = A \cdot e^{\left(-\frac{E_a}{k \cdot T} + B \cdot Q_a\right)} t^z \tag{14}$$

The global approach to identify the model parameters consists in carrying out a linear regression on equation 15. Equation 15 is obtained by applying the logarithm function to equation 14.

$$log(Q_L) = log(A) - \frac{E_a}{k \cdot T} + B \cdot Q_a + z \cdot log(t) \tag{15}$$

Table 2: Identified parameter values: model 2 (section 3.2), models 3 and 3' (section 3.3).

model	z (no units)	A (p.u./day)	B (no units)	E_a (eV)
2	1	$4.35{\cdot}10^7$	1.104	0.719
3	1	$2.31{\cdot}10^9$	1.887	0.834
3′	1	$3.35{\cdot}10^5$	2.154	0.611

This equation represents a hyperplane $w = m + nx + py + qv$ with $w = log(Q_L)$, $x = \frac{1}{T}$, $y = Q_a$ and $v = log(t)$. The parameter identification is easily achieved by a multiple linear regression of experimental data. The identification results for $z = 1$ are collected in table 2 (model 2).

When the parameter values of equation 15 are identified, the next step is to verify the model by comparing simulation to measures. Nevertheless, it is difficult to carry out simulations by using the equation 14 because Q_L and Q_a are coupled in this equation: it is necessary to decouple both variables.

With the relations 4 and 5, Q_a can be expressed as a function of Q_L (equation 16). By plugging 16 in 14, Q_L evolution is no longer dependent of Q_a (equation 17).

$$Q_a = Q_0 - Q_L - Q_d - Q_{sd} \tag{16}$$

$$Q_L = A \cdot e^{\left(-\frac{E_a}{k \cdot T} + B \cdot (Q_0 - Q_L - Q_d - Q_{sd})\right)} t^z \tag{17}$$

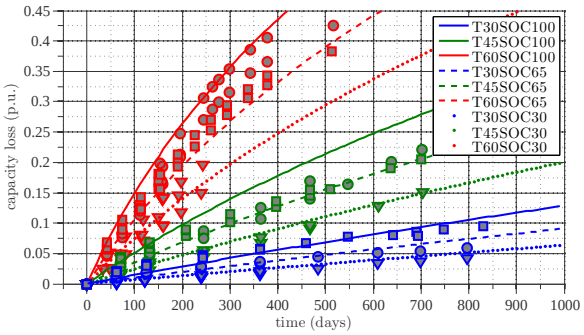
Finally, by assuming $Q_{sd} = 0$ and gathering all the terms depending of Q_L, expression 18 is obtained, where $A' = A \cdot B \cdot e^{BQ_0}$.

$$B \cdot Q_L(t) \cdot e^{B \cdot Q_L(t)} = A' \cdot e^{\left(-\frac{E_a}{k \cdot T} - B \cdot Q_d\right)} t^z \tag{18}$$

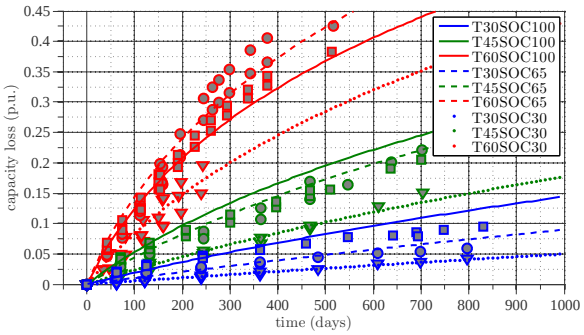
The solution of equation 18 requires to use the Lambert W function. Lambert W function is by definition [23] the solution of the equation $x \cdot e^x = y$ with $x, y \in \mathbb{C}$. In our particular case, y is a real number greater than $-1/e$, so the W_0 branch of the Lambert W function must be used:

$$Q_L(t) = \frac{W_0\left(A' \cdot e^{\left(\frac{-E_a}{k \cdot T}\right)} \cdot e^{(-B \cdot Q_d)} \cdot t^z\right)}{B} \tag{19}$$

Figure 5a shows the simulation results of the model defined by equation 19 with $z = 1$. According to this model, capacity loss trajectory over time will follow the Lambert W function. This result means that in SIMCAL storing conditions (constant T and Q_d), capacity loss evolution is a Lambert function which is between a linear (t) and a squared root of time $\sqrt{t}$.



(a) Model 2, section 3.2: the same model used for SoC100, SoC65 and SoC30



(b) Model 3 (for SoC65 and SoC30) and model 3' (for Soc100), section 3.3.

Figure 5: Simulation results of the model taking into account SoC drift: (a) same model for all SoC values; (b) one model for Soc65 and Soc30, one model for Soc100. Caption for experimental points are the same that in 1.

However, atypical behaviour of SoC100 cells can not be taken into account by this model. As explained above, a particular case without interactions between T and Q_a has been considered (equation 13 with $C = 0$).

3.3. Taking into account of atypical behaviour at SoC100

To improve the model accuracy the atypical behaviour of SoC100 must be considered. As reported in previous works, ageing rate increase at higher levels of *SoC*. But for the experimental results considered in this paper this is true only at 30° C. At 45° C SoC100 ageing is similar to SoC65 and at 60° C ageing is higher for SoC65 cells.

In principle, by adding an interaction term $\frac{C}{kT}$ in the Eyring Law, an additional degree of freedom is added to the model and this would conduct to a better result. The simulations results of the model with interaction term did not show a significant improvement.

Table 3: Description of the models used in the paper: (a) with constant SoC assumption; (b) taking into account the SoC drift.

(a)

Model number	1 & 1'
Equation	$Q_L = A(SoC) \cdot e^{\left(-\frac{E_a(SoC)}{k \cdot T}\right)} t^z$ (8)
Stress factors	T, SoC
Model parameters	A_0, B_S, E_{a0} and C_S
Model constants	k (Boltzmann constant) $z = 0.5$ for model 1 $z = 1$ for model 1'
SoC range	SoC30, 65 and 100

(b)

Model number	2, 3 & 3'
Equation	$Q_L = A \cdot e^{\left(-\frac{E_a}{k \cdot T} + B \cdot Q_a\right)} t^z$ (14)
Stress factors	T, Q_a
Model parameters	A, B, E_a
Model constants	k (Boltzmann constant), $z = 1$
SoC range	model 2: SoC30, 65 and 100 model 3: SoC30, 65 model 3': SoC100

In fact, the voltage of LFP/C cells exhibits an important discontinuity approximately at SoC70 [24]. This discontinuity is the reflection of a phase change in the negative electrode. This would justify that just one Eyring law is not enough, even if an interaction term is used, to model simultaneously ageing of cells in the whole domain of SoC. Therefore, we have modelled SoC100 cells in one side and in the other side SoC65 and SoC30 cells.

The identified model parameter values are collected in the table 2. Model 3 corresponds to SoC65 and SoC30 cells and model 3' to SoC100 cells. Figure 5b shows the simulation results compared to measurements.

4. Results discussion

Table 3 recapitulates the different models used and their main characteristics. Models 1 and 1' use an Arrhenius law with the pre-exponential term (A) and the activation energy (E_a) depending of SoC to take into account the coupling between temperature and SoC. In these models SoC assumed constant during the ageing tests. In model 1 the time function is $\sqrt{t}$ whereas in model 1' time variation is linear. Models 2, 3 and 3' use an Eyring law in order to take into account the SoC drift during the ageing tests. Model 2 attempts to represent the ageing for all values of SoC whereas in models 3 and 3' SoC lower and higher than 70% are considered separately.

Table 4: Simulation error of four models. Models 1 and 1' (section 3.1), model 2 (section 3.2), models 3 and 3' (section 3.3). The minimal values of each line are underlined while maximal values are in bold.

(a) Mean absolute errors (p.u. of nominal capacity).

(T, SoC)	**1 (z=0.5)**	**1' (z=1)**	**2 (z=1)**	**3 and 3' (z=1)**
(30,30)	**0.007**	0.003	0.005	0.002
(30,65)	0.003	0.008	0.005	0.005
(30,100)	0.004	**0.017**	0.010	0.012
(45,30)	**0.026**	0.006	0.006	0.006
(45,65)	**0.024**	0.015	0.008	0.011
(45,100)	0.011	**0.033**	0.030	0.021
(60,30)	**0.021**	0.015	0.015	0.016
(60,65)	**0.052**	0.017	0.034	0.024
(60,100)	0.032	0.023	**0.049**	0.012
mean	**0.020**	0.015	0.018	0.012

(b) Maximum absolute errors (p.u. of nominal capacity).

(T, SoC)	**1 (z=0.5)**	**1' (z=1)**	**2 (z=1)**	**3 and 3' (z=1)**
(30,30)	**0.022**	0.008	0.010	0.004
(30,65)	0.009	0.032	0.015	0.015
(30,100)	0.012	**0.048**	0.014	0.030
(45,30)	**0.082**	0.016	0.016	0.015
(45,65)	**0.081**	0.040	0.023	0.028
(45,100)	0.034	**0.106**	0.074	0.041
(60,30)	**0.059**	0.033	0.031	0.030
(60,65)	0.124	**0.138**	0.089	0.045
(60,100)	0.080	**0.155**	0.130	0.031
maximum	0.124	**0.155**	0.130	0.045

Tables 4a and 4b illustrate the accuracy of each model presented in the previous section. Mean absolute errors (table 4a) show that model 3 is much more accurate than models which do not take into account the SoC drift (40 and 20% better than model 1 and 1' respectively). For model 2, mean errors are 20% lower than for model 1, but mean errors are similar than for model 1'.

Nevertheless, when analysing separately the maximum error values at each test condition (table 4b), a real improvement is visible. For example, at 30° C maximum error of model 2 is under 2% for every SoC, meanwhile for model 1' it is up to 4.8%.

Also, for every test condition, except T30SOC30, the maximum error of model 2 is lower than for the model 1. Finally, model 2 needs one fewer parameter than model 1'.

5. Conclusions

During calendar ageing tests, every factor should be controlled to keep them constant. The two calendar ageing factors are temperature (T) and state-of-charge (SoC). During calendar ageing tests, cells are put in rest condition (disconnected) at a determined temperature and state-of-charge.

When T and SoC are constant, a step-by-step identification may be conducted. For example, calendar ageing model could be expressed with an Arrhenius based equation. In the first step, the temperature influence is identified and give the Arrhenius parameters (A, E_a). In the second step, each parameter is studied as a function of SoC ($A(SoC)$, $E_a(SoC)$).

However, SoC is not constant: SoC drifts over time because of reversible and irreversible capacity losses (Q_{sd} and Q_L). SoC drift must be considered from the parameter identification phase.

By taking into account the SoC drift, all the factors (T, SoC) must be considered at the same time. The global approach shown in this work allows to identify all the parameters at the same time but for this we need to develop the equations and to find an analytical solution beforehand.

The ageing model is based on the Eyring law by taking the couple (T, Q_a) as ageing acceleration factors. In this case, the analytical solution of the equation $x \cdot e^x = y$ is the Lambert W function.

This novel approach results in a significant improvement of the accuracy of the model compared to the classical approach.

It could be applied to any chemistry of batteries. The need of a discontinuity in ageing laws around SoC 70 may be specific to the LFP.

6. Aknowledgement

This work uses data from SIMCAL project. The SIMCAL project (2009-2012) was funded by the French National Research Agency (ANR). SIMCAL partners are CEA, EDF, EIGSI, IFPEN, IFSTTAR, IMS, LEC, LMS-Imagine, LRCS, PSA, RENAULT, SAFT, and VALEO.

References

[1] CGDD, Immatriculations de véhicules neufs et d'occasion en 2014, http://www.statistiques.developpement-durable.gouv.fr/transports/r/immatriculations.html?cHash=dba439ca0c990d713bbfbbd716c06395&tx_ttnews[tt_news]=23978 (2015).
URL http://www.statistiques.developpement-durable.gouv.fr/transports/r/immatriculations.html?cHash=dba439ca0c990d713bbfbbd716c06395&tx_ttnews[tt_news]=23978

[2] M. Natrella, al., NIST/SEMATECH e-handbook of statistical methods, NIST/SEMATECH (2010).
URL http://www.itl.nist.gov/div898/handbook/index.htm

[3] CGDD, enquête nationale transports et déplacements, http://www.statistiques.developpement-durable.gouv.fr/sources-methodes/enquete-nomenclature/1543/139/enquete-nationale-transports-deplacements-entd-2008.html (2008).
URL http://www.statistiques.developpement-durable.gouv.fr/sources-methodes/enquete-nomenclature/1543/139/enquete-nationale-transports-deplacements-entd-2008.html

[4] J. Vetter, P. Novák, M. Wagner, C. Veit, K.-C. Möller, J. Besenhard, M. Winter, M. Wohlfahrt-Mehrens, C. Vogler, A. Hammouche, Ageing mechanisms in lithium-ion batteries, Journal of Power Sources 147 (1 - 2) (2005) 269 – 281. doi:10.1016/j.jpowsour.2005.01.006.
URL http://www.sciencedirect.com/science/article/pii/S0378775305000832

[5] I. Bloom, B. Cole, J. Sohn, S. Jones, E. Polzin, V. Battaglia, G. Henriksen, C. Motloch, R. Richardson, T. Unkelhaeuser, D. Ingersoll, H. Case, An accelerated calendar and cycle life study of li-ion cells, Journal of Power Sources 101 (2) (2001) 238 – 247. doi:10.1016/S0378-7753(01)00783-2.
URL http://www.sciencedirect.com/science/article/pii/S0378775301007832

[6] M. Broussely, S. Herreyre, P. Biensan, P. Kasztejna, K. Nechev, R. Staniewicz, Aging mechanism in li ion cells and calendar life predictions, Journal of Power Sources 97–98 (2001) 13 – 21, proceedings of the 10th International Meeting on Lithium Batteries. doi:10.1016/S0378-7753(01)00722-4.
URL http://www.sciencedirect.com/science/article/pii/S0378775301007224

[7] R. Wright, C. Motloch, J. Belt, J. Christophersen, C. Ho, R. Richardson, I. Bloom, S. Jones, V. Battaglia, G. Henriksen, T. Unkelhaeuser, D. Ingersoll, H. Case, S. Rogers, R. Sutula, Calendar- and cycle-life studies of advanced technology development program generation 1 lithium-ion batteries, Journal of Power Sources 110 (2) (2002) 445 – 470, pNGV. doi:10.1016/S0378-7753(02)00210-0.
URL http://www.sciencedirect.com/science/article/pii/S0378775302002100

[8] A. Eddahech, O. Briat, E. Woirgard, J. Vinassa, Remaining useful life prediction of lithium batteries in calendar ageing for automotive appli-

cations, Microelectronics Reliability 52 (9–10) (2012) 2438 – 2442, ¡ce:title¿SPECIAL {ISSUE} 23rd {EUROPEAN} {SYMPOSIUM} {ON} {THE} {RELIABILITY} {OF} {ELECTRON} DEVICES, {FAILURE} {PHYSICS} {AND} ANALYSIS¡/ce:title¿. doi:10.1016/j.microrel.2012.06.085.
URL http://www.sciencedirect.com/science/article/pii/S002627141200282X

[9] R. Spotnitz, Simulation of capacity fade in lithium-ion batteries, Journal of Power Sources 113 (1) (2003) 72 – 80. doi:10.1016/S0378-7753(02)00490-1.
URL http://www.sciencedirect.com/science/article/pii/S0378775302004901

[10] J. Wang, P. Liu, J. Hicks-Garner, E. Sherman, S. Soukiazian, M. Verbrugge, H. Tataria, J. Musser, P. Finamore, Cycle-life model for graphite-LiFePO4 cells, Journal of Power Sources 196 (8) (2011) 3942–3948. doi:10.1016/j.jpowsour.2010.11.134.
URL http://www.sciencedirect.com/science/article/B6TH1-51KT8D2-3/2/faf150fd8d927be4e1d6b106893b13bc

[11] M. Ecker, N. Nieto, S. Käbitz, J. Schmalstieg, H. Blanke, A. Warnecke, D. U. Sauer, Calendar and cycle life study of li(nimnco)o2-based 18650 lithium-ion batteries, Journal of Power Sources 248 (2014) 839 – 851. doi:10.1016/j.jpowsour.2013.09.143.
URL http://www.sciencedirect.com/science/article/pii/S0378775313016510

[12] O. Tebbi, Estimation des lois de fiabilité en mécanique par les essais accélérés, Ph.D. thesis, Université d'Angers, thèse de Doctorat (2005).
URL https://tel.archives-ouvertes.fr/tel-00009407

[13] A. Delaille, S. Grolleau, F. Duclaud, J. Bernard, R. Revel, S. Pelissier, E. Redondo-Iglesias, J.-M. Vinassa, A. Eddahech, C. Forgez, M. Kassem, S. Joly, D. Porcellato, P. Gyan, S. Bourlot, M. Ouattara-Brigaudet, Simcal project: Calendar aging results obtained on a panel of 6 commercial li-ion cells, in: ECS Meeting Abstracts, no. 14, The Electrochemical Society, San Francisco, 2013, p. 1191.
URL http://ma.ecsdl.org/content/MA2013-02/14/1191.full.pdf

[14] M. Kassem, C. Delacourt, Postmortem analysis of calendar-aged graphite/lifepo4 cells, Journal of Power Sources 235 (2013) 159 – 171. doi:10.1016/j.jpowsour.2013.01.147.
URL http://www.sciencedirect.com/science/article/pii/S037877531300205X

[15] A. Eddahech, O. Briat, J.-M. Vinassa, Strategy for lithium-ion battery performance improvement during power cycling, in: Industrial Electronics Society, IECON 2013 - 39th Annual Conference of the IEEE, 2013, pp. 6806–6811. doi:10.1109/IECON.2013.6700259.

[16] S. Grolleau, A. Delaille, H. Gualous, P. Gyan, R. Revel, J. Bernard, E. Redondo-Iglesias, J. Peter, Calendar aging of commercial graphite/lifepo4 cell – predicting capacity fade under time dependent storage conditions, Journal of Power Sources 255 (2014) 450–458. doi:10.1016/j.jpowsour.2013.11.098.
URL http://www.sciencedirect.com/science/article/pii/S0378775313019411

[17] E. Redondo-Iglesias, P. Venet, S. Pelissier, Influence of the non-conservation of soc value during calendar ageing tests on modelling the capacity loss of batteries, in: Ecological Vehicles and Renewable Energies (EVER), 2015 Tenth International Conference on, Montecarlo, Monaco, 2015, p. 5p. doi:10.1109/EVER.2015.7112987.

[18] M. Ecker, J. B. Gerschler, J. Vogel, S. Käbitz, F. Hust, P. Dechent, D. U. Sauer, Development of a lifetime prediction model for lithium-ion batteries based on extended accelerated aging test data, Journal of Power Sources 215 (2012) 248 – 257. doi:10.1016/j.jpowsour.2012.05.012.
URL http://www.sciencedirect.com/science/article/pii/S0378775312008671

[19] IUPAC, Compendium of Chemical Terminology. Gold book., IUPAC, 2014.
URL http://goldbook.iupac.org/index.html

[20] P. Kreczanik, P. Venet, A. Hijazi, G. Clerc, Study of supercapacitor aging and lifetime estimation according to voltage, temperature, and rms current, Industrial Electronics, IEEE Transactions on 61 (9) (2014) 4895–4902. doi:10.1109/TIE.2013.2293695.

[21] R. German, P. Venet, A. Sari, O. Briat, J.-M. Vinassa, Improved supercapacitor floating ageing interpretation through multipore impedance model parameters evolution, Power Electronics, IEEE Transactions on 29 (7) (2014) 3669–3678. doi:10.1109/TPEL.2013.2279428.

[22] H. Dai, X. Zhang, W. Gu, X. Wei, Z. Sun, A semi-empirical capacity degradation model of ev li-ion batteries based on eyring equation, in: Vehicle Power and Propulsion Conference (VPPC), 2013 IEEE, 2013, pp. 1–5. doi:10.1109/VPPC.2013.6671660.

[23] R. Corless, G. Gonnet, D. Hare, D. Jeffrey, D. Knuth, On the Lambert W function, Advances in Computational Mathematics 5 (1) (1996) 329–359. doi:10.1007/BF02124750.
URL 10.1007/BF02124750

[24] M. A. Roscher, O. Bohlen, J. Vetter, Ocv hysteresis in li-ion batteries including two-phase transition materials, International Journal of Electrochemistry 2011. doi:10.4061/2011/984320.